STAT1 regulates marginal zone B cell differentiation in response to inflammation and infection with blood-borne bacteria

Ting-Ting Chen,[1] Ming-Hsun Tsai,[1] John T. Kung,[2] Kuo-I Lin,[3] Thomas Decker,[4] and Chien-Kuo Lee[1]

[1]Graduate Institute of Immunology, National Taiwan University College of Medicine, Taipei 100, Taiwan
[2]Institute of Molecular Biology and [3]Genomics Research Center, Academia Sinica, Taipei 115, Taiwan
[4]Max F. Perutz Laboratories, University of Vienna, 1030 Vienna, Austria

Marginal zone B (MZ B) cells can rapidly produce antibody in response to infection with blood-borne encapsulated pathogens. Although TLR-mediated activation of MZ B is known to trigger humoral immune response, the signal cascade directing this response remains undefined. Here, we demonstrate that STAT1 plays an essential role in TLR-mediated antibody response of MZ B cells. Further, the TLR-induced IgM response is impaired in a type I and type II IFN-independent manner. Although activation, proliferation, and apoptosis are not affected, both differentiation into plasma cells and IgM production are impaired in *Stat1*$^{-/-}$ MZ B cells. Interestingly, STAT1 directly regulates the expression of *Prdm1* (encodes BLIMP-1) by binding to its promoter, and *Prdm1* expression is reduced in *Stat1*$^{-/-}$ MZ B cells. Restoration of BLIMP-1 to cells rescues TLR-induced IgM response. Moreover, *Stat1*$^{-/-}$ mice are more susceptible to *S. pneumoniae* infection, which can be rescued by the serum of bacteria-primed WT mice. The increased susceptibility to *S. pneumoniae* infection in *Stat1*$^{-/-}$ mice is also intrinsic to STAT1 requirement in MZ B cells. Collectively, these results define a differential regulation of TLR-mediated activation and differentiation of MZ B cells by STAT1 and reveal a STAT1-dependent, but IFN-independent, antibody response during infection and inflammation.

The Journal of Experimental Medicine

INTRODUCTION

Marginal zone B (MZ B) cells are considered to be one of the primary cells responsible for the antibody response to type 2 thymus-independent (TI-2) antigens, such as polysaccharide of encapsulated bacteria (Fagarasan and Honjo, 2000; Martin et al., 2001; Balázs et al., 2002; Oganesyan et al., 2008). To generate rapid responses, MZ B cells have lower thresholds for activation than do follicular B (FO B) cells and are physically poised at the blood–lymphoid interface to facilitate early responses (Martin et al., 2001). Moreover, MZ B cells are described as innate-like B cells in that they express a restricted repertoire of germline-encoded BCRs with polyreactive specificities that bind to multiple microbial molecular patterns (Bendelac et al., 2001; Cerutti et al., 2013). Responding MZ B cells produce an antigen-specific antibody at extrafollicular splenic sites that is low-affinity and predominantly IgM, but also includes limited IgG subclasses. Several lines of evidence suggest that MZ B cells can also mount thymus-dependent (TD) responses and initiate germinal center reactions (Song and Cerny, 2003; Phan et al., 2005).

Once activated, B cells are able to differentiate into antibody-secreting plasma cells. Differentiation of plasma cells from naive B cells is tightly regulated by a network of transcriptional factors, including PAX5, BCL6, BLIMP-1, and XBP1 (Shapiro-Shelef and Calame, 2005). Expression of BCL6 or BLIMP-1 ensures that activated B cells undergo mutually exclusive fates, specifically entering into the germinal center or the plasma cell differentiation pathways, respectively (Shaffer et al., 2002; Vasanwala et al., 2002). BCL6 and BACH2 bind to the promoter of *Prdm1*, a master regulator of plasma cell differentiation, and repress *Prdm1* expression (Shaffer et al., 2000; Tunyaplin et al., 2004; Muto et al., 2010). IRF8 and PU.1 also negatively regulate plasma cell differentiation by concurrently enhancing the expression of *Bcl6* and *Pax5* and repressing *Aicda* (encodes AID) and *Prdm1* (Carotta et al., 2014). IRF4, in contrast, positively regulates class switching recombination (CSR) and plasma cell differentiation by promoting the expression of *Aicda* and *Prdm1* in response to LPS or LPS plus IL-4, respectively (Sciammas et al., 2006). Interestingly, IRF8, PU.1, and IRF4 may bind directly to the same composite sites in the promoters of *Bcl6* and *Prdm1*, thus competing for regulation of the late B cell

Correspondence to Chien-Kuo Lee: leeck@ntu.edu.tw

Abbreviations used: ASC, antibody-secreting cell; ChIP, chromatin immunoprecipitation; CSR, class switching recombination; FO B, follicular B; HK, heat-killed; MZ B, marginal zone B; PC, phosphorylcholine; spB-1a, splenic B-1a; TD, thymus dependent; TI, thymus independent.

The Rockefeller University Press $30.00
J. Exp. Med. 2016 Vol. 213 No. 13 3025–3039
https://doi.org/10.1084/jem.20151620

differentiation (Saito et al., 2007; Carotta et al., 2014). In addition to PU.1 and IRF family members, STAT1 and STAT3 are also involved in B cell differentiation. STAT1 forms complex with Ets-1 and directly regulates the expression of T-bet, which is required for IgG2a production in B cells in response to simultaneous signaling of LPS and IFN-γ or BCR and IFN-γ (Xu and Zhang, 2005; Nguyen et al., 2012). STAT3 activation is sufficient to induce BLIMP-1 expression in primary human B cells in response to IL-21 (Diehl et al., 2008). Interestingly, STAT3 and IRF4 bind to the 3′ region of *Prdm1* in a cooperative manner and promote IL-21–dependent up-regulation of *Prdm1* both in B and T cells (Kwon et al., 2009). Conditional knockout of *Stat3* in the B cell compartment results in selective impairment of TD IgG response (Fornek et al., 2006). However, the mechanisms by which molecules regulate *Prdm1* expression under TI responses remain incompletely understood.

TLR-mediated recognition of microbial stimuli promotes activation and maturation of innate immune cells, including DCs, which instruct and support T cell activation, leading to the cell-mediated adaptive immune response (Akira et al., 2001; Iwasaki and Medzhitov, 2004; Beutler, 2005). Cognate interaction between activated, antigen-specific T cells and naive B cells promotes B cell clonal expansion and differentiation, leading to a humoral immune response. However, accumulated evidence suggests that, in addition to TLR signaling in DCs, direct TLR-mediated activation of B cells is also required to elicit the humoral immune response (Pasare and Medzhitov, 2005). In fact, chimeric mice in which only B cells are deficient in TLR signaling fail to mount antibody responses to protein antigens given with adjuvant. Consistent with this observation, murine B cells can be stimulated in vitro with TLR4 or TLR9 ligands, resulting in antibody secretion (Whitlock and Watson, 1979; Krieg et al., 1995). Although both MZ B and FO B cells express different TLRs, mostly at comparable levels, and respond to their respective agonists, MZ B cells exhibit a greater and faster antibody response than do FO B cells (Oliver et al., 1999; Genestier et al., 2007).

TLR signaling influences TI-2 antibody response by inducing type I IFN (IFN-I), which mediates rapid and significant amounts of antigen-specific IgG2c (Swanson et al., 2010). Although the IgG2c antibody response requires intrinsic IFN-α receptor signaling in B cells, it is independent of TLR signaling. IFN-I also enhances CD138 expression and IgM production, and is required for CpG-mediated IgG2a production (Oganesyan et al., 2008). In addition to IFN-I, IFN-II (or IFN-γ) in combination with BCR signaling regulates class switching to IgG2a, which is mediated by STAT1-dependent induction of T-bet (Xu and Zhang, 2005). STAT1 is a shared signaling mediator of IFN-I and IFN-II signal transduction pathways (Levy and Darnell, 2002). In addition to tyrosine phosphorylation of this molecule on Y701 by Janus kinases, various kinases have been shown to phosphorylate S727 of STAT1, which is required for full transactivation ability of STAT1 (Decker and Kovarik, 2000). In addition to cytokines, UV irradiation and TLRs also induce phosphorylation of this serine in STAT1 through a noncanonical pathway, mediated by p38 MAP kinase (Staab et al., 2013). Moreover, this is MyD88 and TRIF dependent, but IRF3, IRF7, and IFN receptor independent, suggesting that activation is a direct response to TLR ligation rather than to autocrine activation via IFN (Luu et al., 2014). Further, mice with a S727A point mutation display reduced antimicrobial activity and enhanced susceptibility to infection with *Listeria monocytogenes*, emphasizing the importance of this phosphorylation site (Varinou et al., 2003; Pilz et al., 2009).

Despite a well-characterized role of STAT1 in IFN-γ–mediated CSR, the role of STAT1 in the TLR-mediated antibody response remains elusive. In this study, we demonstrate the differential regulation of activation and differentiation of MZ B cells by STAT1 in response to TLR stimulation and bacterial infection. We also define a STAT1-dependent, but IFN-independent, antibody response occurring through the direct regulation of *Prdm1* expression.

RESULTS

Impaired IgM response in *Stat1*$^{-/-}$ MZ B cells in response to TLR stimulation

B cells, including B-1, MZ B, and FO B cells, express TLRs. Moreover, they proliferate and differentiate into IgM-producing plasma cells in response to stimulation by various TLR agonists (Genestier et al., 2007). To investigate the molecular mechanisms underlying the TLR-mediated activation and differentiation of B cells, we studied the involvement of STAT1, a shared mediator of IFN-I and IFN-II signaling, in MZ B and FO B cells, two major B2 subsets in the spleen. To this end, MZ B and FO B cells of WT and *Stat1*$^{-/-}$ mice were stimulated with various TLR ligands, including Pam_3CSK_4, LPS, R848, and CpG ODN 1826. Although both MZ B and FO B cells were activated and produced IgM in response to TLR stimulation, the titers of IgM produced by MZ B cells were approximately 10-fold higher than those produced by FO B cells (Fig. 1, A and B). This enhanced response by MZ B cells is consistent with results of a previous study (Genestier et al., 2007). Interestingly, TLR-induced IgM production was significantly reduced in *Stat1*$^{-/-}$ MZ B cells compared with WT MZ B cells after stimulation, although the impaired response was also observed, to a lesser extent, in FO B cells when using R848 and CpG, but not LPS and Pam_3CSK_4, as stimuli. To examine whether the defect in IgM production by *Stat1*$^{-/-}$ MZ B cells is dependent on IFN-I or IFN-II, MZ B cells from WT, *Ifnar1*$^{-/-}$, and *Ifngr1*$^{-/-}$ mice, respectively, were stimulated with the same TLR agonists. TLR-induced IgM production from WT, *Ifnar*$^{-/-}$, or *Ifngr*$^{-/-}$ MZ B cells was comparable (Fig. 1, C and D), suggesting that the impaired IgM response in *Stat1*$^{-/-}$ MZ B cells is IFN-I or IFN-II independent.

The role of STAT1 in the IgM response was further examined in vivo. WT or *Stat1*$^{-/-}$ mice were stimulated with LPS in vivo and serum IgM was measured. As shown

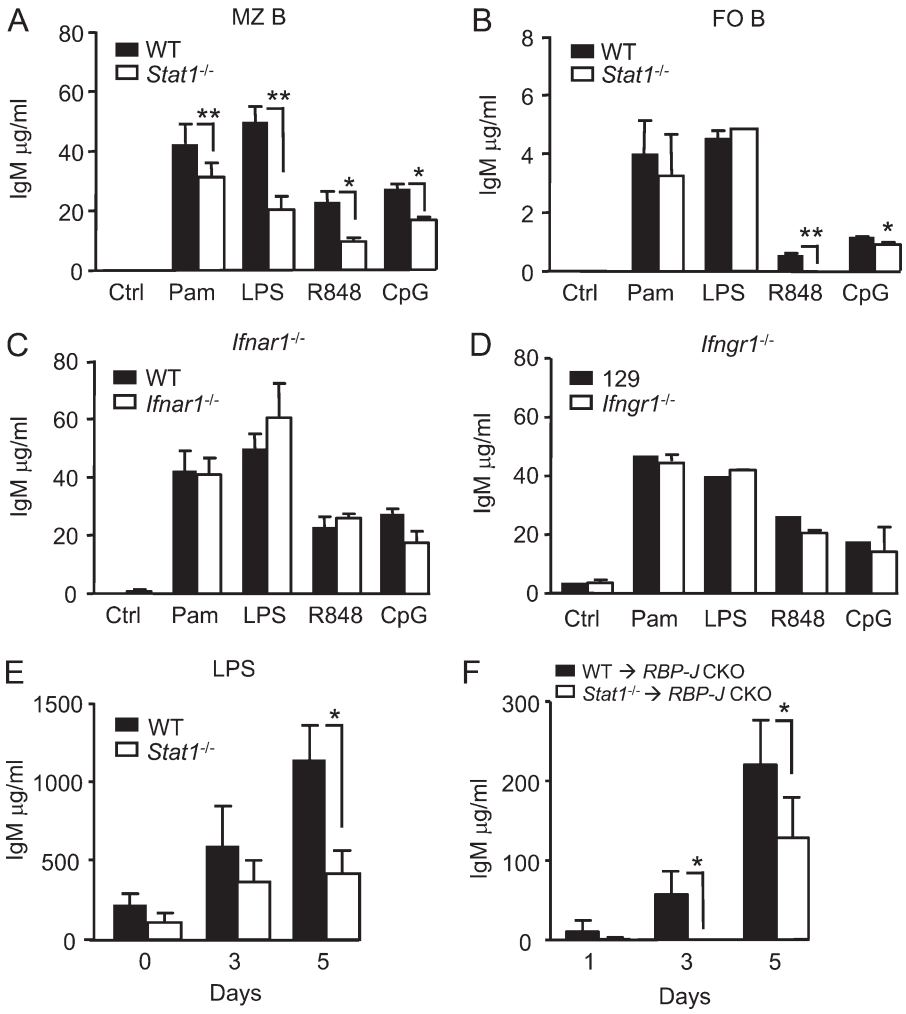

Figure 1. **Impaired IgM response in *Stat1*$^{-/-}$ MZ B cells in response to TLR stimulation in vitro and in vivo.** MZ B (A) or FO B (B) cells of WT and *Stat1*$^{-/-}$ mice were treated with or without 1 µg/ml Pam3CSK4 (Pam), 2 µg/ml LPS, 10 µg/ml R848, or 1 µg/ml CpG for 4 d (n = 3–5). Results represent three experiments. Same as in A, except MZ B cells of WT and (C) *Ifnar1*$^{-/-}$ or (D) *Ifngr1*$^{-/-}$ mice were stimulated with the indicated TLR agonists for 4 d. Secreted IgM in the culture supernatant was measured by ELISA (n = 2–5). Results represent two to three experiments. (E) WT and *Stat1*$^{-/-}$ mice were intravenously injected with 25 µg LPS for 0, 3, and 5 d (n = 5). Results represent three experiments. (F) MZ B cells of WT or *Stat1*$^{-/-}$ mice (2×10^6 each) were adoptively transferred into RBP-J CKO mice for 1 d, and then 25 µg LPS was intravenously injected for the indicated times. Total serum IgM of the treated mice was measured by ELISA (n = 4). Results represent two experiments. All values are shown as the means ± SD. *, $P < 0.05$; **, $P < 0.01$, Student's t test.

in Fig. 1 E, after stimulation for 5 d, production of IgM was significantly reduced in *Stat1*$^{-/-}$ mice. To study whether the impaired IgM response was intrinsic to STAT1 requirement in MZ B cells, we performed adoptive transfer experiments. MZ B cells from WT or *Stat1*$^{-/-}$ mice were transferred into CD19-Cre x *RBP-J*$^{f/f}$ conditional KO (RBP-J CKO) mice, in which MZ B cell development is severely impaired (Tanigaki et al., 2002), and stimulated with LPS. Reduced IgM production was still observed in mice receiving *Stat1*$^{-/-}$ MZ B cells in contrast to those with WT MZ B cells, suggesting that the defect in LPS-induced IgM production in *Stat1*$^{-/-}$ mice is MZ B cell autonomous (Fig. 1 F).

STAT1 affects TLR-induced plasma cell differentiation but not activation, proliferation, or apoptosis of MZ B cells

To investigate the mechanisms underlying the impaired IgM response of *Stat1*$^{-/-}$ mice, we first examined whether the generation of MZ B cells was affected by STAT1. As shown in Fig. 2 (A and B), the percentages and numbers of splenic MZ B cells are comparable between WT and *Stat1*$^{-/-}$ mice. Moreover, the impaired IgM response in *Stat1*$^{-/-}$ MZ B cells in response to CpG is not a result of reduced TLR9 expression, as it is equally expressed on both cell types both before and after stimulation (unpublished data). Consistent with this result, increased doses of CpG could not rescue the defect in *Stat1*$^{-/-}$ MZ B cells (unpublished data). We next examined the effect of STAT1 on the TLR-induced response in MZ B cells. Up-regulation of CD69 and MHC class II on MZ B cells from WT or *Stat1*$^{-/-}$ mice stimulated with or without CpG or LPS were found to be similar (Fig. 2, C–F). Likewise, induction of IL-6 was also comparable (Fig. 2 G), although IL-10 levels were slightly decreased in *Stat1*$^{-/-}$ MZ B cells upon LPS, but not CpG, stimulation (Fig. 2 H). TLR-mediated proliferation and apoptosis, as revealed by BrdU incorporation and Annexin V staining, respectively, were similar between WT and *Stat1*$^{-/-}$ MZ B cells (Fig. 2, I and J).

Because activation, proliferation, and apoptosis of MZ B cells were not affected by the loss of STAT1, we next examined plasma cell differentiation. MZ B cells from WT or *Stat1*$^{-/-}$ mice were stimulated with CpG or LPS and differentiation into plasma cell was assessed. The percentage of plasma cells ($B220^{-}CD138^{+}$) derived from *Stat1*$^{-/-}$ MZ B

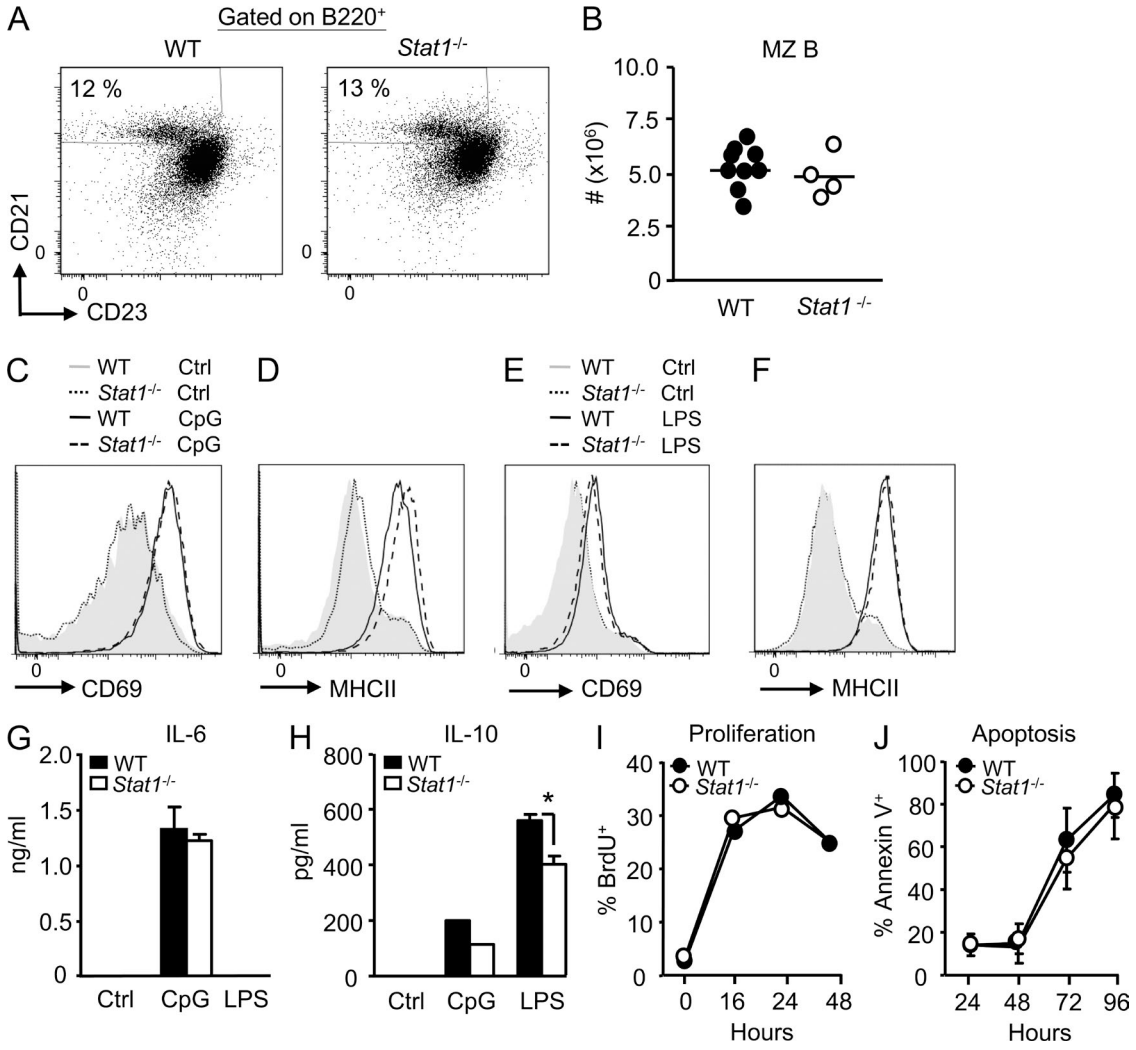

Figure 2. **Development and TLR-induced activation, proliferation, and apoptosis of *Stat1*$^{-/-}$ MZ B cells are normal.** (A) Splenocytes of WT and *Stat1*$^{-/-}$ mice were stained with antibodies to B220, CD21, and CD23, gated on B220, and analyzed for MZ B cells (B220^{+}CD21^{hi}CD23^{lo}) by flow cytometry. One experiment out of three is shown. (B) Mean numbers of WT and *Stat1*$^{-/-}$ MZ B cells are shown (n = 4–9). Results represent three experiments. (C–F) MZ B cells of WT and *Stat1*$^{-/-}$ mice were stimulated with 1 µg/ml CpG (C and D) or 2 µg/ml LPS (E and F) for 24 h, stained with antibodies to CD69 (C and E) and MHC class II (D and F), respectively, and analyzed by flow cytometry. One experiment out of two is shown. (G and H) Same as in C–F, except the culture supernatant of the stimulated cells were subjected to ELISA for measuring the production of IL-6 (G) and IL-10 (H) before and after the treatments (n = 2). Results represent two experiments. (I) Same as in A and B except cells were stimulated for the indicated times, pulsed with BrdU for the last 2 h, and stained with anti–BrdU-FITC, and then BrdU incorporation measured by flow cytometry. One experiment out of two is shown. (J) Same as in I except the cells were treated for the indicated times, stained with Annexin V, and analyzed with flow cytometry (n = 3). Results represent three experiments. All values are shown as the means ± SD. *, P < 0.05, Student's t test.

cells was reduced compared with that from WT MZ B cells (Fig. 3, A–C). Similarly, the frequencies of antibody-secreting cells (ASCs), as determined by ELISPOT, were also reduced in the absence of STAT1 (Fig. 3, D and E). However, the mean spot size, indicating antibody-secreting ability of each ASC, was comparable (Fig. 3 F). To further decipher the potential mechanisms underlying the differentiation defect of *Stat1*$^{-/-}$ MZ B cells, we measured the expression of genes that are critical for controlling differentiation processes, such as *Pax5*, *Bcl6*, *Prdm1*, and *Xbp1s* (spliced form of *Xbp1*). As expected, expression of *Pax5* and *Bcl6* was found to be decreased, whereas *Prdm1* and *Xbp1s* were increased in both cell types after LPS stimulation for 2 d. Interestingly, the expression of *Prdm1* and *Xbp1s* in stimulated *Stat1*$^{-/-}$ MZ B cells was lower than in WT MZ B cells, although *Pax5* and *Bcl6* were comparable (Fig. 3, G–J). A similar result was also observed in CpG-stimulated MZ B cells (unpublished data). Together, these results suggest that STAT1 does not affect the homeostasis or TLR-induced activation, proliferation, or apoptosis of MZ B cells. Instead,

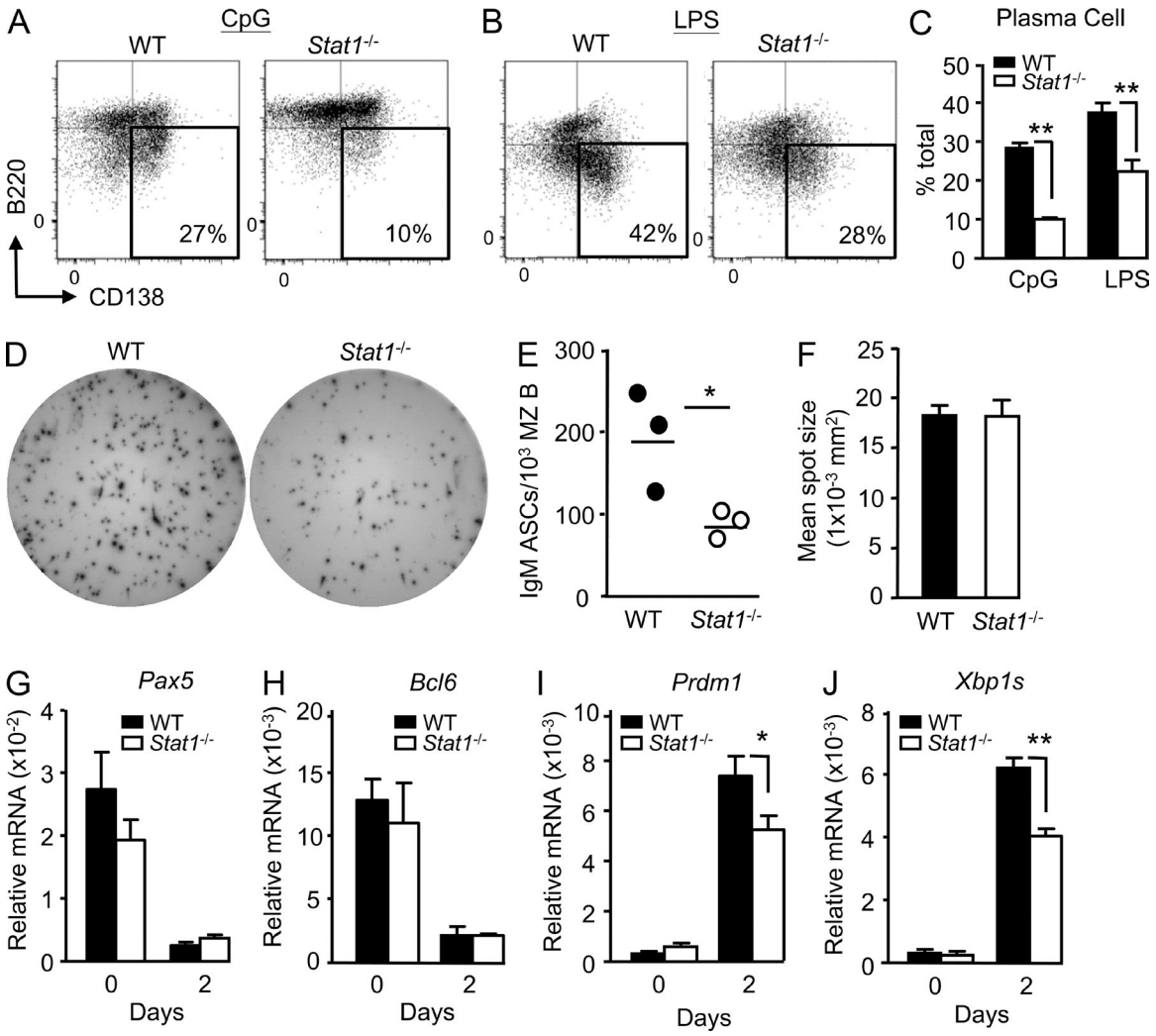

Figure 3. **Impaired plasma cell differentiation in *Stat1*$^{-/-}$ MZ B cells in response to TLR stimulation.** MZ B cells of WT and *Stat1*$^{-/-}$ mice were stimulated with 1 µg/ml CpG (A) and 2 µg/ml LPS (B), respectively, for 2 d, stained with antibodies to B220 and CD138, and analyzed by flow cytometry. One experiment out of three is shown. (C) The mean percentages of plasma cell (B220^{-}CD138^{+}) after stimulation are shown ($n = 3$). Results represent three experiments. MZ B cells were stimulated with 1 µg/ml CpG for 3 d, and then subjected to ELISPOT assay. (D) The spots of ASCs are shown. One experiment out of three is shown. The frequencies of ASCs per 10^3 MZ B cells (E) and mean area of each spot (F) in the ELISPOT assay is shown ($n = 3$). Results represent three experiments. Same as in B, except mRNA was prepared from the cells before and after stimulation with LPS and subjected to RT-QPCR using primers to *Pax5* (G), *Bcl6* (H), *Prdm1* (I), and *Xbp1s* (J). All genes were normalized to *Rpl7* ($n = 4$). Results represent two experiments. All values are shown as the means ± SD. *, $P < 0.05$; **, $P < 0.01$, Student's *t* test.

STAT1 affects the differentiation process, probably through regulation of *Prdm1* and/or *Xbp1s*.

STAT1 positively regulates *Prdm1* expression and restoration of BLIMP-1 rescues the impaired IgM response in *Stat1*$^{-/-}$ MZ B cells

It is known that *Prdm1* expression is regulated by IRF4 (Sciammas et al., 2006) and IRF8-PU.1 (Carotta et al., 2014) in a reciprocal manner. Therefore, we first examined the expression of these three molecules and found that their levels were comparable between WT and *Stat1*$^{-/-}$ MZ B cells before and after CpG stimulation (unpublished data), suggesting that STAT1 might regulate *Prdm1* in an IRF4- or IRF8-independent manner. To confirm the essential role of STAT1 in the IgM response, we knocked down *Stat1* in CH12F3, a mouse B cell line. As expected, LPS-stimulated IgM production and *Prdm1* expression were significantly lower in the *Stat1* knockdown cells compared with the *luciferase* knockdown control (Fig. 4, A and B). We next examined whether STAT1 directly regulates the expression of *Prdm1* or *Xbp1s*. We first did in silico analysis for the STAT1 ChIP-seq database (Robertson et al., 2007) and found that IFN-γ–activated STAT1 was capable of binding to the *Prdm1* loci (Fig. 4 C), but not to the *Xbp1* loci (not depicted). We next performed a

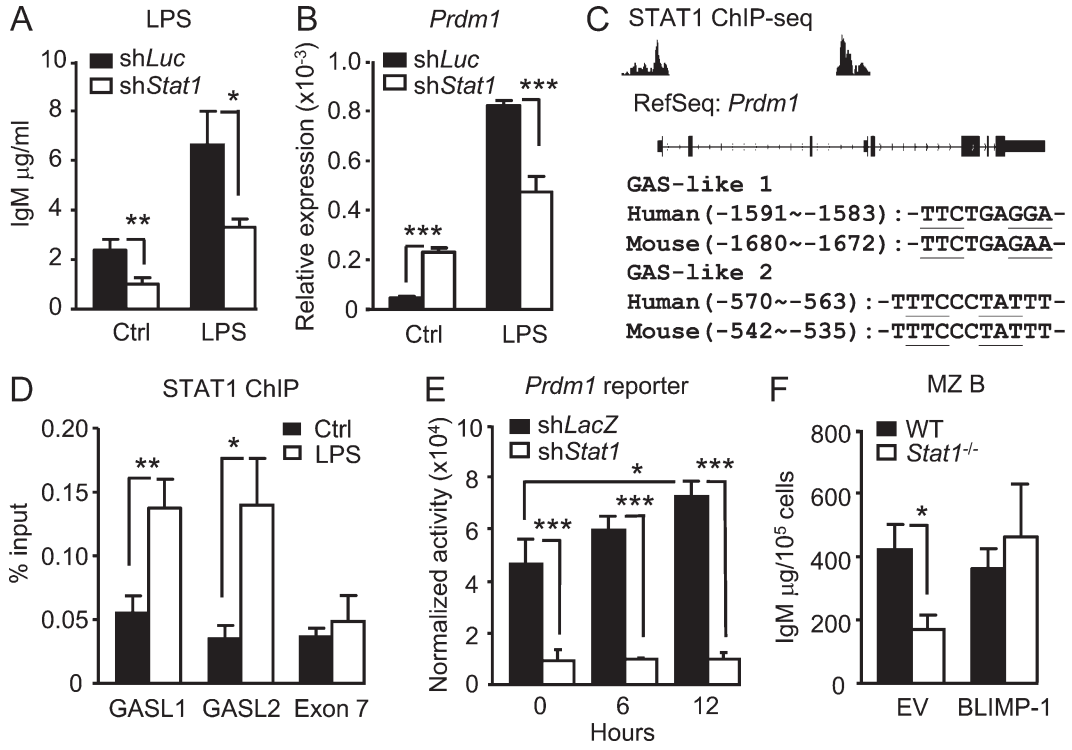

Figure 4. **STAT1 binds to *Prdm1* promoter and regulates *Prdm1* expression and IgM production in MZ B cells in response to TLR stimulation.** (A) CH12F3 cells were subjected to lentivirus-based knockdown of *luciferase* or *Stat1*, and then stimulated with or without LPS for 4 d. IgM in the culture supernatant was measured by ELISA ($n = 3$). Results represent three experiments. (B) Same as in A, except total RNA from the cells treated for 2 d were subjected to RT-QPCR using primers to *Prdm1* ($n = 6$). Results represent three experiments. (C) ChIP-seq data (Robertson et al., 2007) were analyzed for STAT1 binding regions in human *Prdm1* loci. The corresponding exons and introns of *Prdm1* are shown. Comparison of conserved GAS-like 1 (GASL1) and GAS-like 2 (GASL2) in human and mouse *Prdm1* promoters are shown. (D) CH12F3 cells were stimulated with 5 µg/ml LPS for 6 h, and ChIP was performed using anti-STAT1 antibody. Relative abundance of GASL1 (A), GASL2 (B), and exon 7 are shown ($n = 6$). Results represent three experiments. (E) Reporter plasmid containing the promoter region of *Prdm1* (−2,052 to +207 bp) was cotransfected with pCMV-DsRed, an internal control plasmid, into sh*LacZ*- or sh*Stat1*-treated CH12F3 cells for 24 h, followed by stimulation with 5 µg/ml LPS for the indicated times before being harvested and subjected to reporter activity assay. Reporter activity was normalized to the percentage of DsRed-positive cells ($n = 3$). Results represent three experiments. (F) MZ B cells from WT or *Stat1*$^{-/-}$ mice were stimulated with 2 µg/ml LPS for 24 h and transduced with recombinant retrovirus pGC-YFP or pGC-Blimp-1-YFP for 2 d. The YFP^{+} cells were sorted out and incubated for another 24 h before measuring IgM production by ELISA ($n = 3$). Results represent three experiments. All values are shown as the means ± SD *, $P < 0.05$; **, $P < 0.01$; ***, $P < 0.001$, Student's *t* test.

ChIP assay to verify the direct binding of STAT1 to two potential IFN-γ–activated sequences (GAS) that are conserved between human and mouse *Prdm1* promoters, namely GAS-like 1 and GAS-like 2 (Fig. 4 C). STAT1 was indeed able to bind to these two sites in response to LPS stimulation in CH12F3 cells, whereas STAT1 did not bind to exon 7, which does not contain a GAS (Fig. 4 D). These results suggest that, upon stimulation, STAT1 is able to bind directly to the *Prdm1* promoter. Moreover, the activity of a luciferase reporter was attenuated in LPS-stimulated CH12F3 in which *Stat1* had been knocked down (Fig. 4 E). Together, these results suggest that STAT1 directly binds to the promoter of *Prdm1* and is critical for its expression in response to LPS. We next examined whether restoration of BLIMP-1 in *Stat1*$^{-/-}$ MZ B cells is able to rescue the IgM response (Fig. 4 F). Indeed, a BLIMP-1–expressing plasmid, and not an empty vector control, was able to rescue the production of IgM in *Stat1*$^{-/-}$ MZ B cells in response to LPS stimulation. In sum, STAT1 positively regulates *Prdm1* expression in MZ B cells, which is essential for the IgM response to TLR stimulation.

Stat1$^{-/-}$ mice are more susceptible to blood-borne *S. pneumoniae* infection

The early antibody response from MZ B cells plays a critical role in host defense against extracellular encapsulated bacteria, such as *S. pneumoniae* (Martin et al., 2001), which are recognized by different innate sensors, including TLR2 and TLR4 for cell wall components and TLR9 for CpG-containing DNA (Koppe et al., 2012). Therefore, we next examined the significance of the STAT1-dependent IgM response in MZ B cells during *S. pneumoniae* infection. MZ B cells from WT and *Stat1*$^{-/-}$ mice were first stimulated in vitro with heat-killed (HK) *S. pneumoniae*. WT MZ B cells were activated and produced IgM in a dose-dependent manner; whereas the

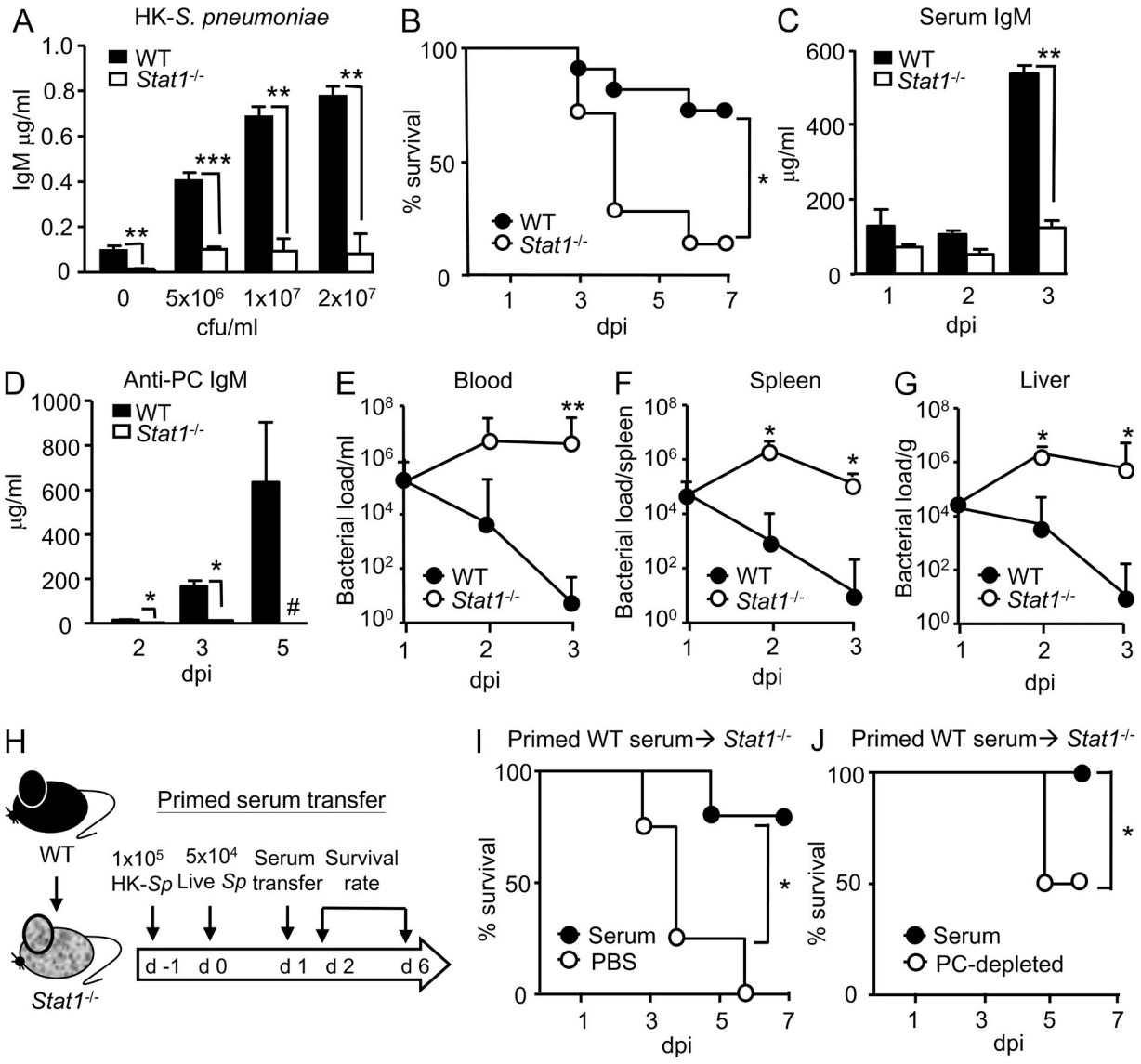

Figure 5. **Impaired IgM response and increased susceptibility to *S. pneumoniae* infection in *Stat1*$^{-/-}$ mice.** (A) MZ B cells of WT and *Stat1*$^{-/-}$ mice were stimulated with the indicated doses of HK-*S. pneumoniae* in vitro for 4 d, and IgM in the culture supernatant was measured by ELISA. Results represent three experiments. (B) WT and *Stat1*$^{-/-}$ mice were primed with intravenous injection of 10^5 CFU HK-*S. pneumoniae* for 24 h before being challenged with a lethal dose of 5×10^4 live *S. pneumoniae*. Survival curves for WT and *Stat1*$^{-/-}$ mice are shown. dpi, days postinfection ($n = 7$). Results represent two experiments. (C and D) Same as in B, except serum IgM (C) and anti-PC IgM (D) was measured by ELISA at the indicated times ($n = 3$). # mice died. Results represent two experiments. (E–G) Same as in B, except bacterial load in the blood (E), spleen (F), and liver (G) was measured ($n = 3$–5). Results represent three experiments. (H) Schematic diagram of serum transfer to *Stat1*$^{-/-}$ mice from WT mice that had been primed with *S. pneumoniae*. (I) PBS or primed serum from WT mice was transferred into *Stat1*$^{-/-}$ mice 1 d after infection with 5×10^4 CFU of live *S. pneumoniae* ($n = 4$–6). Results represent two experiments. (J) Same as in I, except serum from primed WT mice were either untreated or PC-depleted first, and then transferred into *Stat1*$^{-/-}$ mice. Survival curves are shown ($n = 7$). Results represent three experiments. All values are shown as the means ± SD. *, $P < 0.05$; **, $P < 0.01$; ***, $P < 0.001$, Student's *t* test (A and C–G) or Log-rank test (B, I, and J).

IgM response of *Stat1*$^{-/-}$ MZ B cells was significantly lower (Fig. 5 A). Because both MZ B and B-1 cells are splenic innate-like B cells (Martin and Kearney, 2001), we specifically examined the role of MZ B cells in *S. pneumoniae* infection in vivo using RBP-J CKO mice in which development of MZ B cells is severely impaired (Tanigaki et al., 2002). The mice were first primed with HK-*S. pneumoniae*, followed by challenge with a lethal dose of live *S. pneumoniae*. RBP-J CKO mice were indeed more susceptible to *S. pneumoniae* infection than WT mice (unpublished data). We next compared the susceptibility of WT and *Stat1*$^{-/-}$ mice under the same treatments. The survival rate of *Stat1*$^{-/-}$ mice was significantly

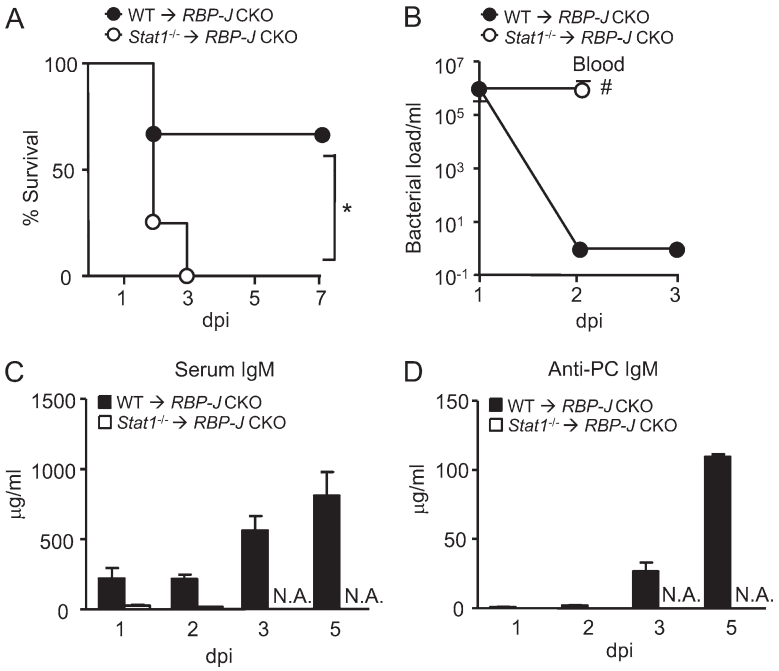

Figure 6. **Increased susceptibility to *S. pneumoniae* infection in *Stat1*$^{-/-}$ mice is intrinsic to the loss of STAT1 in MZ B cells.** (A) MZ B cells sorted from WT and *Stat1*$^{-/-}$ mice were intravenously transferred into RBP-J CKO mice. 1 d later, chimeric mice were primed with 10^5 CFU HK-*S. pneumoniae* for 1 d before being challenged with a lethal dose of 10^3 live *S. pneumoniae*. Survival curves are shown. dpi, days postinfection (n = 5–6). Results represent three experiments. (B) Same as in A, except bacterial loads in the blood were measured (n = 3–6). # mice died. Results represent three experiments. (C and D) Same as in A, except serum total IgM and PC-specific IgM were measured by ELISA at the indicated times (n = 3–6). Results represent two experiments. All values are shown as the means ± SD. *, P < 0.05, Log-rank test (A) or Student's t test (B–D).

lower than that of WT mice (Fig. 5 B), which coincided with the reduced serum IgM titers in *Stat1*$^{-/-}$ mice (Fig. 5 C). It has been shown that IgM against phosphorylcholine (PC), an important cell wall component of *S. pneumoniae*, plays a critical role in resistance to *S. pneumoniae* infection (Wallick et al., 1983). Thus, we next examined the levels of anti-PC IgM and found that these antibodies were induced in WT mice and peaked at 5 d after infection, whereas in contrast, anti-PC IgM was barely detectable in *Stat1*$^{-/-}$ mice after the infection (Fig. 5 D). The bacterial loads in the peripheral blood, spleen, and liver of *Stat1*$^{-/-}$ mice were also higher (Fig. 5, E–G). These results suggest that decreased IgM response in *Stat1*$^{-/-}$ mice may account for the increased susceptibility to *S. pneumoniae* infection. To confirm this possibility, we performed serum transfer experiments. A schematic diagram of the serum transfer procedure is shown in Fig. 5 H. In brief, HK-*S. pneumoniae*–primed serum from WT mice was transferred to *Stat1*$^{-/-}$ mice that had been primed with HK-*S. pneumoniae* and then challenged with a lethal dose of live *S. pneumoniae*. Indeed, the primed serum from WT mice was able to protect *Stat1*$^{-/-}$ mice from lethal infection (Fig. 5 I). Further, the protective effect of the primed serum was attenuated after the depletion of anti-PC antibody (Fig. 5 J), suggesting that the decreased anti-PC antibody in *Stat1*$^{-/-}$ mice might account for the increased susceptibility to *S. pneumoniae* infection.

Increased susceptibility to *S. pneumoniae* infection in *Stat1*$^{-/-}$ mice is intrinsic to STAT1 requirement in MZ B cells

To further confirm the requirement of STAT1 in MZ B cells during *S. pneumoniae* infection, we did adoptive transfer experiments. MZ B cells of WT and *Stat1*$^{-/-}$ mice were first intravenously transferred into RBP-J CKO mice. After the priming of these chimeric mice with HK-*S. pneumoniae*, they were infected with a lethal dose of live *S. pneumoniae* (1,000 CFU for RBP-J CKO mice). The mice receiving *Stat1*$^{-/-}$ MZ B cells were indeed more susceptible to *S. pneumoniae* infection than those receiving WT MZ B cells (Fig. 6 A), with sustained bacterial loads and died 2 d later, whereas the mice receiving WT MZ B cells were able to clear the bacteria and survived (Fig. 6 B). Total IgM and PC-specific IgM were also detected in chimeric mice receiving WT MZ B cells, but not in those receiving *Stat1*$^{-/-}$ MZ B cells after the infection (Fig. 6, C and D). These results suggest that the increased susceptibility to *S. pneumoniae* infection in *Stat1*$^{-/-}$ mice is intrinsic to the requirement of STAT1 in MZ B cells in vivo.

TLR- and *S. pneumoniae*–stimulated serine phosphorylation of STAT1 contributes to the IgM response in MZ B cells

Because STAT1 regulates TLR-induced IgM response in MZ B cells, we next examined whether STAT1 is activated by TLR agonists in these cells. Although CpG- or LPS-stimulated phosphorylation of STAT1 S727 and Y701, phosphorylation of S727 was more pronounced when compared with IFN-α stimulation (Fig. 7, A and B). To study the involvement of STAT1 S727 phosphorylation in the TLR-induced IgM response, WT mice or *Stat1*$^{SA/SA}$ mice, in which the serine at position 727 was mutated into alanine, were stimulated with LPS in vivo. After stimulation for 5 d, IgM levels were decreased in the sera of *Stat1*$^{SA/SA}$ mice compared with WT mice (Fig. 7 C), although the impairment was less severe than that of *Stat1*$^{-/-}$ mice receiving the same treatment (Fig. 1 E). To confirm the impaired IgM response in *Stat1*$^{SA/SA}$ mice was

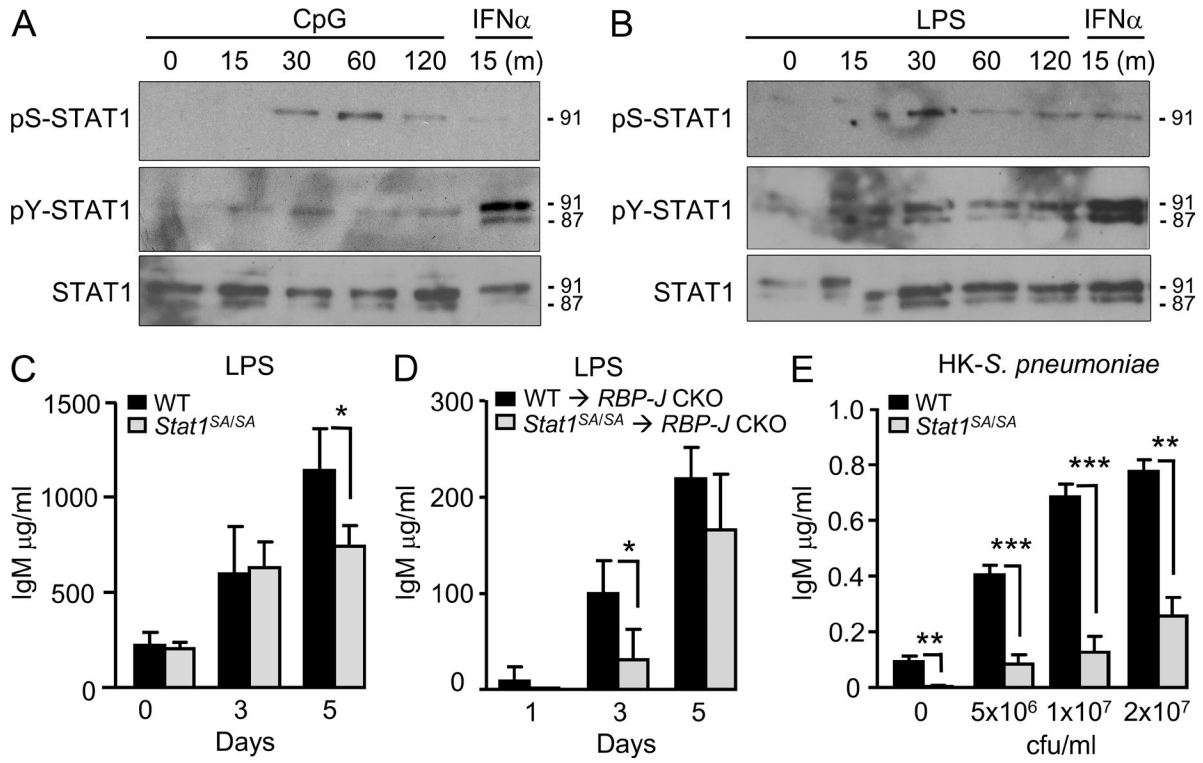

Figure 7. **Serine phosphorylation of STAT1 regulates IgM production from MZ B cells.** MZ B cells of WT mice were stimulated with 10 µg/ml CpG (A), 10 µg/ml LPS (B), or 1,000 U/ml IFN-α4 for the indicated times. Cell extracts were analyzed by immunoblotting with antibodies to serine- or tyrosine-phosphorylated STAT1 (pS-STAT1 or pY-STAT1) and STAT1. One experiment out of three is shown. (C) WT and *Stat1*$^{SA/SA}$ mice were intravenously injected with 25 µg LPS and IgM in the serum was measured by ELISA at the indicated times (n = 6–11). Results represent three experiments. (D) MZ B cells of WT or *Stat1*$^{SA/SA}$ mice (2×10^6 each) were transferred into RBP-J CKO mice for 1 d, and then 25 µg LPS was intravenously injected. Total serum IgM of the mice treated at the indicated times was measured by ELISA (n = 3). Results represent three experiments. (E) MZ B cells of WT and *Stat1*$^{SA/SA}$ mice were stimulated with the indicated doses of HK-*S. pneumoniae* in vitro for 4 d, and IgM in the culture supernatant was measured by ELISA (n = 4). Results represent four experiments. All values are shown as the means ± SD. *, P < 0.05; **, P < 0.01; ***, P < 0.001, Student's t test.

intrinsic to MZ B cells, adoptive transfer was performed. Indeed, after stimulation for 3 d, IgM titers were also reduced in RBP-J CKO mice receiving MZ B cells of *Stat1*$^{SA/SA}$ mice compared with WT controls (Fig. 7 D). Nevertheless, the defect in the IgM response eventually recovered after 5 d of the treatment. Decreased IgM production was also observed in *Stat1*$^{SA/SA}$ MZ B cells when stimulated with HK-*S. pneumoniae* in vitro (Fig. 7 E). Nevertheless, *Stat1*$^{SA/SA}$ mice did not show increased susceptibility to *S. pneumoniae* infection compared with WT mice (unpublished data). Together, these results suggest that S727 phosphorylation of STAT1 partially contributes to positive regulation of the inflammation- and infection-induced IgM response in MZ B cells.

DISCUSSION

We have demonstrated that STAT1 regulates TLR-mediated plasma cell differentiation and IgM production, but not activation, proliferation, or apoptosis of MZ B cells. Although STAT1 is a shared molecule for type I and type II IFN signaling pathways, both of which are involved in CSR and antibody response (Le Bon et al., 2001; Peng et al., 2002), the effect of STAT1 in the IgM response is independent of both IFNs. Interestingly, STAT1 also regulates pristane-mediated autoantibody production in a manner distinct from IRF9 or IFN-I receptor signaling (Thibault et al., 2008, 2009). Although *Irf9*$^{-/-}$ or *Ifnar2*$^{-/-}$ mice show hyper-IgM syndrome as a result of a general block in CSR after pristane challenge, *Stat1*$^{-/-}$ mice display reduced IgM levels after the stimulation. In fact, we have also reported a distinct requirement of STAT1 and IFNs for NK activity (Lee et al., 2000).

Accumulated evidence suggests that two major signaling pathways may regulate the activation of STATs, including STAT1: the canonical pathway induced by cytokine receptors and JAKs, and the noncanonical pathway triggered by cell stress (UV), TLR, TNF receptor, etc. (Decker and Kovarik, 2000; Bezbradica and Schroder, 2014). TLR, for example, can use noncanonical pathway to directly activate STAT1 by S727 phosphorylation independent of autocrine IFN-I signaling (Luu et al., 2014). Indeed, STAT1 was phosphorylated on S727 in addition to Y701 in MZ B cells in response to LPS or CpG stimulation. The magnitude of TLR-stimulated S727 phosphorylation is greater than that stimulated by IFN-I re-

ceptor. Interestingly, S727 phosphorylation also contributes to the TLR-induced IgM response in MZ B cells, as mutation of this site in STAT1 (S727A) resulted in reduced IgM production in response to LPS stimulation in vivo and HK-*S. pneumoniae* treatment in vitro. However, the mutant mice did not show significant defects upon live *S. pneumoniae* challenge in vivo, suggesting that phosphorylation of S727 is not sufficient and that phosphorylation of Y701 on STAT1 or STAT1 protein itself is necessary to mount competent antibody response during infection. S727 phosphorylation of STAT1 is also known to regulate macrophage and NK cell activities (Varinou et al., 2003; Putz et al., 2013), and IFN-γ–mediated antiviral response in MEFs (Bancerek et al., 2013). *Stat1*$^{SA/SA}$ mutant mice are more susceptible to *L. monocytogenes* infection and exhibit impaired clearance of this pathogen (Varinou et al., 2003). In contrast, NK cells from *Stat1*$^{SA/SA}$ mutant mice display enhanced cytotoxicity against a range of tumors, accompanied by increased expression of perforin and Granzyme B (Putz et al., 2013). Thus, STAT1 S727 phosphorylation appears to control various immune responses in a cell type–specific manner.

A predominant role of the STAT1-dependent antibody response in MZ B cells is early host defense against infection with blood-borne encapsulated bacteria. We have demonstrated that STAT1 is required for triggering the IgM response in MZ B cells in response to *S. pneumoniae* in vitro and in vivo. Moreover, the levels of total or PC-specific IgM were also significantly reduced in *Stat1*$^{-/-}$ mice, which resulted in a failure of bacterial clearance and increased susceptibility to intravenous infection with *S. pneumoniae*. Interestingly, the impaired IgM response in *Stat1*$^{-/-}$ MZ B cells in vitro and *Stat1*$^{-/-}$ mice in vivo was much more severe in response to *S. pneumoniae* than to TLR stimulation. One possibility for this is that the defect becomes more obvious with suboptimal stimulation. Indeed, the difference in IgM production between WT and *Stat1*$^{-/-}$ MZ B cells at lower doses of CpG stimulation was greater than at higher doses (unpublished data). Moreover, the amount of IgM induced by HK-*S. pneumoniae* in vitro was ∼1–5% of that induced by TLR ligation, which mimicked low-dose TLR stimulation. Alternatively, STAT1 may be involved in signaling downstream of multiple pattern recognition receptors from *S. pneumoniae*, of which the TLR response represents only one type. Although STAT1 is essential for host responses to viral or intracellular bacterial infections, such as *Listeria* or *Mycobacteria* (Boisson-Dupuis et al., 2012), this is, to our knowledge, the first example that STAT1 also plays a role in clearance of extracellular bacteria.

One mechanism for STAT1-dependent regulation of the antibody response is transcriptional control of BLIMP-1, the master regulator of plasma cell differentiation. We have shown that TLR-activated STAT1 binds to two conserved GAS-like elements in the promoter region of BLIMP-1. Reporter assays further suggest that the regulatory elements encompassing these two sites control the expression of *Prdm1* in a STAT1-dependent manner. Of note, GASL2 is a potential composite binding site for IRFs and PU.1, which are known to bind to 5′ promoter and 3′ regulatory element of *Prdm1* and regulate its expression during TD responses (Carotta et al., 2014). However, GASL1 and GASL2 are located in a distinct 5′ promoter region of *Prdm1*. Because IRF4 has been shown to cooperate with STAT3 to regulate *Prdm1* expression through binding to two GAAA-containing sites downstream of the GAS (Kwon et al., 2009), further experiments will be required to determine if there is cooperativity between IRF4 and STAT1 to promote *Prdm1* expression.

In addition to MZ B cells, B-1 cells are also known to play a role in the early humoral response against *S. pneumoniae* infection (Martin and Kearney, 2001; Haas et al., 2005). Both MZ B and B-1 cells are found in the spleen, and are capable of producing protective, anti-PC antibodies against *S. pneumoniae* (Haas et al., 2005). However, MZ B cells have a more diverse repertoire and are able to interact with a wider variety of blood-borne antigens. MZ B cells can also be constantly replenished from bone marrow, which contrasts with the very limited renewal capacity of B-1 cells in the adult (Martin et al., 2001). Therefore, MZ B cells and B-1 cells may play distinct roles in antibody responses to different TI bacterial antigens. Although we cannot exclude the involvement of B-1 cells in the impaired IgM response and increased susceptibility to *S. pneumoniae* infection in *Stat1*$^{-/-}$ mice in vivo, we still believe the role of MZ B cells to be crucial because a similar phenotype was observed in RBP-J CKO mice (unpublished data), which have intact B-1 cells (Tanigaki et al., 2002) or in the RBP-J CKO chimeric mice receiving *Stat1*$^{-/-}$ MZ B cells. Surprisingly, the percentages and numbers of splenic B-1a (spB-1a) were increased in *Stat1*$^{-/-}$ mice as compared with WT control (unpublished data). LPS-induced *Prdm1* expression and IgM production, however, was still lower in *Stat1*$^{-/-}$ spB-1a cells (unpublished data). Because WT and *Stat1*$^{-/-}$ mice had comparable numbers of peritoneal B-1a and B-1b (unpublished data), the enhanced frequency of spB-1a in *Stat1*$^{-/-}$ mice is probably not a general effect on B-1 cells. Together, STAT1 regulates the differentiation of both MZ B and spB-1a cells, and appears to be critical for innate-like humoral immune response.

Naturally occurring antibodies against the PC determinant of the pneumococcal cell wall C-carbohydrate in the normal mouse serum is found to be crucial for the protection of intravenous infection with *S. pneumoniae* (Briles et al., 1981b). Passive administration of IgG3 against PC or type 3 pneumococcal polysaccharide protects mice from *S. pneumoniae* infection (Briles et al., 1981a). Moreover, the protective effect of antigen-specific IgG3 is even better than that of antigen-specific IgM. The production of serum IgG was markedly enhanced in WT mice after *S. pneumoniae* infection for 1 d and was further increased after 3 d. However, *Stat1*$^{-/-}$ mice produced significantly lower amount of serum IgG as opposed to WT control (unpublished data). Similarly, production of PC-specific IgG was also found to be reduced in the absence of STAT1 (unpublished data). Together, these results suggest that STAT1 regulates the production of natural

antibodies, including PC-specific IgM and IgG in response to TLR stimulation or blood-borne bacterial infection.

In the current study, we demonstrate the requirement for STAT1 in MZ B cells for TLR- or blood-borne bacteria-induced IgM response. This is in agreement with human studies showing a reduction of IgM in some patients with autosomal-dominant, heterozygous STAT1 mutations, despite them having normal numbers of $CD19^+CD20^+$ B cells (Sharfe et al., 2014). Because polyreactive MZ B and B-1 cells account for many of the B cells expressing self-reactivity in the periphery, improper regulation of these B cells may be an important factor contributing to autoimmune diseases (Martin and Kearney, 2002; Pillai et al., 2005; Duan and Morel, 2006).

MATERIALS AND METHODS

Mice

All mice used in this study are on the C57BL/6 background except *Ifngr1*$^{-/-}$ mice, which are on 129 background (Huang et al., 1993). WT mice were purchased from the National Laboratory Animal Center (NLAC), Taiwan. All other mice, including *Stat1*$^{-/-}$ (Durbin et al., 1996), *Ifnar1*$^{-/-}$ (Chen et al., 2013), *Ifngr1*$^{-/-}$, and *Stat1*$^{SA/SA}$ (Varinou et al., 2003) mutant mice were bred and kept under specific pathogen–free conditions in the Laboratory Animal Center, National Taiwan University College of Medicine. RBP-J CKO mice (Tanigaki et al., 2002) were provided by T. Honjo (Kyoto University, Kyoto, Japan). The use of the animals was reviewed and approved by the Institutional Animal Care and Use Committee of National Taiwan University College of Medicine (permit number: 20120075).

Antibodies and flow cytometry

Cell staining was performed at 4°C with Fc Block (hybridoma 2.4G2) in FACS staining buffer (0.5% FBS and 0.1% NaN_3 in dPBS). Anti–B220-FITC, anti–B220-PE, anti–CD21-APC, Annexin V-FITC, anti–BrdU-FITC, and Streptavidin-PE were purchased from BioLegend. Anti–CD23-biotin and anti–CD138-biotin were purchased from BD. Anti–CD69-biotin, anti–MHC-II-PE, and anti–TLR9-FITC were purchased from eBioscience. Flow data were acquired by the FACSCanto II (BD) and analyzed by FlowJo software.

Cell sorting, cell culture, and adoptive transfer

Splenocytes were stained with anti–B220-FITC, anti–CD21-APC, anti–CD23-biotin, and Streptavidin-PE at 4°C for 10 m. MZ B ($B220^+CD21^{hi}CD23^{lo}$) and FO B cells ($B220^+CD21^{int}CD23^{hi}$) were sorted using the FACSAria IIIu (BD). MZ B cells and FO B cells (10^5/well) were cultured in 200 µl complete RPMI medium (RPMI 1640 medium supplemented with 10% FBS, 10 µg/ml gentamycin, and 50 µM β-ME) at 37°C 5% CO_2 humidified incubator in 96-well U-bottom plates. TLR agonists, including 1 µg/ml Pam_3CSK_4 (InvivoGen), 2 µg/ml LPS (Sigma-Aldrich), 10 µg/ml R848 (Enzo Life Sciences), and 1 µg/ml CpG ODN 1826 (Sigma-Aldrich), were used to stimulate B cells in vitro for 4 d. For adoptive transfer experiments, 2–3 × 10^6 sorted WT or *Stat1*$^{-/-}$ MZ B cells were intravenously injected into RBP-J CKO mice. In LPS stimulation experiments, the chimeric mice were intravenously injected with 25 µg LPS 1 d after the transfer.

ELISA

Purified MZ B and FO B cells were cultured at 10^5 cells in 200 µl complete RPMI medium. Supernatants were harvested at d 4, and IgM levels were measured by ELISA. In brief, 96-well MaxiSorb plates (Nunc) were coated with 5 µg/ml goat anti–mouse IgM (H + L) antibodies (Southern Biotech) overnight at 4°C. The plates were washed, and then blocked with 3% BSA in PBS for 60 m at room temperature. Supernatants were diluted and added to the plates along with purified mouse IgM control (Southern Biotech) as a standard. The plates were incubated for 60 m at room temperature, then washed, and goat anti–mouse IgM was conjugated to HRP (1:5,000; Southern Biotech) were added and incubated for 60 m. TMB substrate was added, and then stopped by 100 µl 2N H_2SO_4. OD_{450} were measured with a microplate reader and analyzed (Molecular Devices). IL-6 was measured by ELISA MAX Deluxe Sets (BioLegend). IL-10 was measured by Mouse IL-10 DuoSet (R&D Systems). For anti-PC antibody, 5 µg/ml PC-BSA (Bioresearch Technologies) was coated onto 96-well plates before the assay.

Activation, proliferation, and apoptosis assays

For the activation assay, 10^5 cells/ml MZ B cells were stimulated with 1 µg CpG ODN 1826 or 2 µg/ml LPS for 24 h, and then analyzed by flow cytometry for the up-regulation of CD69 and MHC class II. For the proliferation assay, purified MZ B cells were pulsed with 10 µg/ml BrdU for 2 h before harvest at the indicated times. Cells were fixed and permeabilized with 1 ml of 1% formaldehyde and 0.01% Tween 20 in PBS and incubated at 4°C overnight, and then were washed and resuspended in PBS containing Ca^{2+} and Mg^{2+} and digested with 50,000 U DNaseI (Sigma-Aldrich) at 37°C for 30 min. Cells were washed once with PBS and resuspended in 50 µl of PBS containing 10% BSA and 0.5% Tween 20, and then stained with 5 µl anti-BrdU antibody at room temperature for 30 min and subjected to FACS analysis. For the apoptosis assay, sorted MZ B cells were treated with TLR agonists for the indicated times, followed by staining with Annexin V-FITC according to the manufacturer's instructions.

ELISPOT assay

Purified MZ B cells and FO B cells were cultured at 10^5 cells/200 µl complete RPMI medium as described in the Cell sorting, cell culture, and adoptive transfer section. After 48 h of culture, cells were washed and distributed at various concentrations into Multiscreen HTS plates (EMD Millipore) precoated with 10 µg/ml goat anti–mouse IgM (H + L; Southern Biotech) in 2% FBS RPMI 1640 medium, and then incubated for 24 h at 37°C in 5% CO_2. Plates were washed, and then incubated with biotin-conjugated goat anti–mouse IgM (H + L; 1:5,000; Southern Biotechnology Associates) for

2 h at room temperature. Plates were washed, and then treated with alkaline phosphatase–conjugated Streptavidin (1:1,000; Sigma-Aldrich) and developed with 5-bromo-4-chloro-3-indoyl phosphate/NBT (Sigma-Aldrich). ISCs were enumerated using the KS ELISPOT (ZEISS).

Quantitative RT-PCR

The mRNA was isolated from purified MZ B cells from WT and *Stat1*$^{-/-}$ mice stimulated with or without 1 μg/ml CpG ODN 1826 and 2 μg/ml LPS, respectively, for 2 d and cDNA was synthesized using the TurboCapture 96 mRNA kit (QIAGEN). Quantitative real-time PCR was performed using the PikoReal detection system (Thermo Fisher Scientific) using primers to *Pax5*, *Bcl6*, *Prdm1*, *Xbp1s*, and *Rpl7*. Data were analyzed by PikoReal Software 2.0. The results were normalized to *Rpl7*.

In silico analysis

STAT1 ChIP-seq raw data (STAT1_hg18_IFNg_ht11.wig.gz and STAT1_hg18_Unstimulated_ht11.wig.gz) were downloaded from supplementary data 1 (Robertson et al., 2007). The files were first unzipped to .wig files and were converted to a binary tiled data (.tdf) files using the Integrative Genomics Viewer (IGV) program. The .wig.tdf files were opened in the IGV program, and the ChIP-seq results on the loci of *Prdm1* and *Xbp1* were analyzed.

RNA silencing

The lentiviruses carrying short hairpin RNA (shRNA) targeting STAT1, LacZ, and luciferase were purchased from the National RNAi Core Facility (Institute of Molecular Biology/Genomics Research Center, Academia Sinica, Taiwan). The core facility is part of The RNAi Consortium. The sequence targeting mouse STAT1 is 5′-GCTGTTACTTTCCCAGATATT-3′ (TRCN0000054926), and the control constructs targeting LacZ and luciferase are 5′-CGCGATCGTAATCACCCGAGT-3′(TRCN0000072224) and 5′-CAAATCACAGAATCGTCGTAT-3′ (TRCN0000072246), respectively. 4×10^4 CH12F3 cells were infected with lentivirus at an MOI of 10–50, with 8 μg/ml polybrene by spin infection 1,100 *g* for 50 min at room temperature. 2 d after the infection, the cells were cultured in a selection medium containing 0.5 μg/ml puromycin for 7 d to enrich infected cells before experiments were performed.

ChIP assay

The ChIP protocol was adapted from the fast protocol (Nelson et al., 2006), with some modifications. In brief, cells were fixed in 1.42% formaldehyde at room temperature, followed by quenching with 125 mM glycine. Cells were washed with cold PBS, collected, and pelleted by centrifugation at 2,000 *g* for 5 min. Cells were then resuspended in nuclei lysis buffer (0.05 M Tris, 0.01 M EDTA, 1% SDS, 1 mM PMSF, and 1× protease inhibitor cocktail), and then incubated on ice for 10 min to lyse the nuclei. Nuclear extracts were then sonicated with Vibra-Cell VCX 130 sonicator (Sonics and Materials, Inc.) to obtain 200–500-bp fragments of chromatin. The sonication conditions were 15 s on and 45 s off on ice for 15 min. For immunoprecipitation, protein A beads (Roche) conjugated with anti-STAT1 antibody (made in-house; Wang et al., 2011) were added to nuclear extracts and incubated overnight. The immune complexes were then washed with the following buffers; three times with ChIP buffer (50 mM NaCl, 50 mM Tris-HCl, pH 7.5, 5 mM EDTA, 0.5% NP-40, 1% Triton X-100, 0.5 mM PMSF, 10 mM NaF, and 0.1 mM Na_3VO_4), once with high-salt wash buffer (same as ChIP buffer except 500 mM NaCl), LiCl wash buffer (same as ChIP buffer except 150 mM NaCl and an additional 300 mM LiCl), and ChIP buffer. The chromatin was eluted with freshly prepared elution buffer (1% SDS, and 50 mM $NaHCO_3$), followed by reverse cross-linking with 0.3 M NaCl at 67°C overnight. The samples were incubated with 20 μg proteinase K in proteinase K buffer (10 mM Tris, pH 7.5, 5 mM EDTA, and 0.25% SDS) at 55°C for 4 h to degrade protein. DNA was then recovered by phenol-chloroform extraction and ethanol precipitation. Recovered DNA from ChIP was analyzed by quantitative PCR using primers as shown below.

Reporter assay

The promoter region of *Prdm1* from −2,052 bp to approximately +207 bp (Tunyaplin et al., 2000) was PCR amplified using template DNA of CH12F3 (T. Honjo, Kyoto University) cells (Muramatsu et al., 2000) and cloned into pGL4.32 using restriction enzyme sites KpnI and HindIII. The reporter plasmid (4 μg) and pCMV-DsRed (1 μg), an internal control, were transiently transfected into CH12F3, which had been knocked down by sh*LacZ* or sh*Stat1*, using 4D-Neucleofactor System (Lonza) according to the manufacturer's instructions. The transfection efficiency was ∼7–14%, as indicated by DsRed-positive cells using flow cytometry. After transfection for 24 h, the cells were stimulated with or without 5 μg/ml LPS for an additional 6 or 12 h before being harvested. Luciferase activity was measured by the ONE-Glo Luciferase Assay Substrate (Promega) with an EnVision 2103 Multilabel Reader (PerkinElmer). Firefly luciferase activity was normalized to percentage of DsRed-positive cells.

Retroviral transduction

The procedure for preparing viral vectors was as previously described (Lin et al., 2007). For pseudotyped virus, retroviral vector pGC-YFP or pGC-Blimp-1-YFP (15 μg), pSV-Ψ$^-$E-MLV (15 μg), and VSV-G (pMD.G; 15 μg) were transfected into 293T cells. The viral supernatants were collected 2 d later and concentrated by ultracentrifugation (Beckman Coulter) at 25,000 rpm for 90 m. MZ B cells were stimulated with 2 μg/ml LPS for 24 h, and then transduced with retrovirus by spin infection at 1,100 *g* for 50 m, with an MOI of 10, in RPMI 1640 containing 10% FBS and 8 μg/ml of poly-

brene (Sigma-Aldrich). After retroviral transduction for 2 d, YFP^+ cells were sorted out and were further incubated for 24 h. The culture supernatant was collected for measuring IgM production by ELISA.

Priming and challenging of *S. pneumoniae*

WU-2L strain *S. pneumoniae* (provided by D.E. Briles, University of Alabama, Birmingham, AL) was grown in Brain and Heart infusion broth and was frozen as glycerol stocks at −80°C. At the time of infection, bacteria were diluted in sterile PBS for intravenous injection, and the number of CFU injected was reconfirmed by enumerating colony growth on blood agar plates (BAP). Heat-killed *S. pneumoniae* were generated by incubating bacteria at 100°C for 30 m, with death confirmed by the absence of growth in BAP. For WT or *Stat1*$^{-/-}$ mice, 10^5 CFU HK-*S. pneumoniae* were intravenously injected to prime the mice. 1 d later, the mice were challenged with 5×10^4 CFU lethal dose of live bacteria. For adoptively transferred chimeric mice, the procedure was the same, except HK-*S. pneumoniae* were injected into the mice 1 d after the transfer of MZ B cells. Moreover, 10^3 lethal doses of live bacteria were used to challenge the mice. Bacterial loads of each recipient were measured by plating blood, spleen, or liver samples on BAP.

Western blotting

Sorted MZ B cells (5×10^5) were left untreated or treated with 10 µg/ml LPS, 10 µg/ml CpG ODN 1826, or 1,000 U IFN-α4 for 1 h. Cells were lysed in IP lysis buffer (300 mM NaCl, 50 mM Hepes, pH 7.6, 1.5 mM $MgCl_2$, 10% glycerol, 1% Triton X-100, 10 mM NaPyrPO4, 20 mM NaF, 1 mM EGTA, and 0.1 mM EDTA) plus freshly added 1 mM DTT, 1 mM PMSF, 10 µl proteinase inhibitor cocktail (Sigma-Aldrich), 1 mM Na_3VO_4, and 20 mM NaF. Primary antibodies pS727-STAT1 (Cell Signaling Technology) and pY701-STAT1 (Cell Signaling Technology) and STAT1 (made in-house) were used.

Statistical analyses

All values are shown as mean ± STDEV. Two-tailed, paired, or homoscedastic Student's *t* test was used to assess statistical significance. Log-rank (Mantel-Cox) test was used to assess statistical significance of survival rate. *, $P < 0.05$; **, $P < 0.01$; and ***, $P < 0.001$.

Online supplemental material

Table S1 shows primer sequences used for real-time QPCR. Table S2 shows primer sequences used for ChIP.

ACKNOWLEDGMENTS

We are grateful to Drs. Tasuku Honjo, Guann-Yi Yu, David Briles, Yi-Ping Chuang, and Ming-Jiun Yu for providing reagents and experimental assistance and the seventh Core Laboratory at National Taiwan University Hospital for providing equipment. We also acknowledge the service provided by the Flow Cytometric Analysis and Cell Sorting Core Facility of the First Core Laboratory at National Taiwan University College of Medicine.

This work was supported by the Ministry of Science and Technology, Taiwan (MOST 102-2320-B-002-030-MY3) and the National Health Research Institutes, Taiwan (NHRI-EX102-10256SI and NHRI-EX103-10256SI).

The authors declare no competing financial interests.

Submitted: 12 October 2015
Revised: 24 August 2016
Accepted: 19 October 2016

REFERENCES

Akira, S., K. Takeda, and T. Kaisho. 2001. Toll-like receptors: critical proteins linking innate and acquired immunity. *Nat. Immunol.* 2:675–680. http://dx.doi.org/10.1038/90609

Balázs, M., F. Martin, T. Zhou, and J. Kearney. 2002. Blood dendritic cells interact with splenic marginal zone B cells to initiate T-independent immune responses. *Immunity.* 17:341–352. http://dx.doi.org/10.1016/S1074-7613(02)00389-8

Bancerek, J., Z.C. Poss, I. Steinparzer, V. Sedlyarov, T. Pfaffenwimmer, I. Mikulic, L. Dölken, B. Strobl, M. Müller, D.J. Taatjes, and P. Kovarik. 2013. CDK8 kinase phosphorylates transcription factor STAT1 to selectively regulate the interferon response. *Immunity.* 38:250–262. http://dx.doi.org/10.1016/j.immuni.2012.10.017

Bendelac, A., M. Bonneville, and J.F. Kearney. 2001. Autoreactivity by design: innate B and T lymphocytes. *Nat. Rev. Immunol.* 1:177–186. http://dx.doi.org/10.1038/35105052

Beutler, B. 2005. The Toll-like receptors: analysis by forward genetic methods. *Immunogenetics.* 57:385–392. http://dx.doi.org/10.1007/s00251-005-0011-3

Bezbradica, J.S., and K. Schroder. 2014. TRAF6 is a nexus for TLR-STAT1 crosstalk. *Immunol. Cell Biol.* 92:737–738. http://dx.doi.org/10.1038/icb.2014.71

Boisson-Dupuis, S., X.F. Kong, S. Okada, S. Cypowyj, A. Puel, L. Abel, and J.L. Casanova. 2012. Inborn errors of human STAT1: allelic heterogeneity governs the diversity of immunological and infectious phenotypes. *Curr. Opin. Immunol.* 24:364–378. http://dx.doi.org/10.1016/j.coi.2012.04.011

Briles, D.E., J.L. Claflin, K. Schroer, and C. Forman. 1981a. Mouse Igg3 antibodies are highly protective against infection with Streptococcus pneumoniae. *Nature.* 294:88–90. http://dx.doi.org/10.1038/294088a0

Briles, D.E., M. Nahm, K. Schroer, J. Davie, P. Baker, J. Kearney, and R. Barletta. 1981b. Antiphosphocholine antibodies found in normal mouse serum are protective against intravenous infection with type 3 streptococcus pneumoniae. *J. Exp. Med.* 153:694–705. http://dx.doi.org/10.1084/jem.153.3.694

Carotta, S., S.N. Willis, J. Hasbold, M. Inouye, S.H. Pang, D. Emslie, A. Light, M. Chopin, W. Shi, H. Wang, et al. 2014. The transcription factors IRF8 and PU.1 negatively regulate plasma cell differentiation. *J. Exp. Med.* 211:2169–2181. http://dx.doi.org/10.1084/jem.20140425

Cerutti, A., M. Cols, and I. Puga. 2013. Marginal zone B cells: virtues of innate-like antibody-producing lymphocytes. *Nat. Rev. Immunol.* 13:118–132. http://dx.doi.org/10.1038/nri3383

Chen, Y.L., T.T. Chen, L.M. Pai, J. Wesoly, H.A. Bluyssen, and C.K. Lee. 2013. A type I IFN-Flt3 ligand axis augments plasmacytoid dendritic cell development from common lymphoid progenitors. *J. Exp. Med.* 210:2515–2522. http://dx.doi.org/10.1084/jem.20130536

Decker, T., and P. Kovarik. 2000. Serine phosphorylation of STATs. *Oncogene.* 19:2628–2637. http://dx.doi.org/10.1038/sj.onc.1203481

Diehl, S.A., H. Schmidlin, M. Nagasawa, S.D. van Haren, M.J. Kwakkenbos, E. Yasuda, T. Beaumont, F.A. Scheeren, and H. Spits. 2008. STAT3-mediated up-regulation of BLIMP1 Is coordinated with BCL6 down-regulation

to control human plasma cell differentiation. *J. Immunol.* 180:4805–4815. http://dx.doi.org/10.4049/jimmunol.180.7.4805

Duan, B., and L. Morel. 2006. Role of B-1a cells in autoimmunity. *Autoimmun. Rev.* 5:403–408. http://dx.doi.org/10.1016/j.autrev.2005.10.007

Durbin, J.E., R. Hackenmiller, M.C. Simon, and D.E. Levy. 1996. Targeted disruption of the mouse Stat1 gene results in compromised innate immunity to viral disease. *Cell.* 84:443–450. http://dx.doi.org/10.1016/S0092-8674(00)81289-1

Fagarasan, S., and T. Honjo. 2000. T-Independent immune response: new aspects of B cell biology. *Science.* 290:89–92. http://dx.doi.org/10.1126/science.290.5489.89

Fornek, J.L., L.T. Tygrett, T.J. Waldschmidt, V. Poli, R.C. Rickert, and G.S. Kansas. 2006. Critical role for Stat3 in T-dependent terminal differentiation of IgG B cells. *Blood.* 107:1085–1091. http://dx.doi.org/10.1182/blood-2005-07-2871

Genestier, L., M. Taillardet, P. Mondiere, H. Gheit, C. Bella, and T. Defrance. 2007. TLR agonists selectively promote terminal plasma cell differentiation of B cell subsets specialized in thymus-independent responses. *J. Immunol.* 178:7779–7786. http://dx.doi.org/10.4049/jimmunol.178.12.7779

Haas, K.M., J.C. Poe, D.A. Steeber, and T.F. Tedder. 2005. B-1a and B-1b cells exhibit distinct developmental requirements and have unique functional roles in innate and adaptive immunity to S. pneumoniae. *Immunity.* 23:7–18. http://dx.doi.org/10.1016/j.immuni.2005.04.011

Huang, S., W. Hendriks, A. Althage, S. Hemmi, H. Bluethmann, R. Kamijo, J. Vilcek, R.M. Zinkernagel, and M. Aguet. 1993. Immune response in mice that lack the interferon-gamma receptor. *Science.* 259:1742–1745. http://dx.doi.org/10.1126/science.8456301

Iwasaki, A., and R. Medzhitov. 2004. Toll-like receptor control of the adaptive immune responses. *Nat. Immunol.* 5:987–995. http://dx.doi.org/10.1038/ni1112

Koppe, U., N. Suttorp, and B. Opitz. 2012. Recognition of Streptococcus pneumoniae by the innate immune system. *Cell. Microbiol.* 14:460–466. http://dx.doi.org/10.1111/j.1462-5822.2011.01746.x

Krieg, A.M., A.K. Yi, S. Matson, T.J. Waldschmidt, G.A. Bishop, R. Teasdale, G.A. Koretzky, and D.M. Klinman. 1995. CpG motifs in bacterial DNA trigger direct B-cell activation. *Nature.* 374:546–549. http://dx.doi.org/10.1038/374546a0

Kwon, H., D. Thierry-Mieg, J. Thierry-Mieg, H.P. Kim, J. Oh, C. Tunyaplin, S. Carotta, C.E. Donovan, M.L. Goldman, P. Tailor, et al. 2009. Analysis of interleukin-21-induced Prdm1 gene regulation reveals functional cooperation of STAT3 and IRF4 transcription factors. *Immunity.* 31:941–952. http://dx.doi.org/10.1016/j.immuni.2009.10.008

Le Bon, A., G. Schiavoni, G. D'Agostino, I. Gresser, F. Belardelli, and D.F. Tough. 2001. Type i interferons potently enhance humoral immunity and can promote isotype switching by stimulating dendritic cells in vivo. *Immunity.* 14:461–470. http://dx.doi.org/10.1016/S1074-7613(01)00126-1

Lee, C.K., D.T. Rao, R. Gertner, R. Gimeno, A.B. Frey, and D.E. Levy. 2000. Distinct requirements for IFNs and STAT1 in NK cell function. *J. Immunol.* 165:3571–3577. http://dx.doi.org/10.4049/jimmunol.165.7.3571

Levy, D.E., and J.E. Darnell Jr. 2002. Stats: transcriptional control and biological impact. *Nat. Rev. Mol. Cell Biol.* 3:651–662. http://dx.doi.org/10.1038/nrm909

Lin, F.R., H.K. Kuo, H.Y. Ying, F.H. Yang, and K.I. Lin. 2007. Induction of apoptosis in plasma cells by B lymphocyte-induced maturation protein-1 knockdown. *Cancer Res.* 67:11914–11923. http://dx.doi.org/10.1158/0008-5472.CAN-07-1868

Luu, K., C.J. Greenhill, A. Majoros, T. Decker, B.J. Jenkins, and A. Mansell. 2014. STAT1 plays a role in TLR signal transduction and inflammatory responses. *Immunol. Cell Biol.* 92:761–769. http://dx.doi.org/10.1038/icb.2014.51

Martin, F., and J.F. Kearney. 2001. B1 cells: similarities and differences with other B cell subsets. *Curr. Opin. Immunol.* 13:195–201. http://dx.doi.org/10.1016/S0952-7915(00)00204-1

Martin, F., and J.F. Kearney. 2002. Marginal-zone B cells. *Nat. Rev. Immunol.* 2:323–335. http://dx.doi.org/10.1038/nri799

Martin, F., A.M. Oliver, and J.F. Kearney. 2001. Marginal zone and B1 B cells unite in the early response against T-independent blood-borne particulate antigens. *Immunity.* 14:617–629. http://dx.doi.org/10.1016/S1074-7613(01)00129-7

Muramatsu, M., K. Kinoshita, S. Fagarasan, S. Yamada, Y. Shinkai, and T. Honjo. 2000. Class switch recombination and hypermutation require activation-induced cytidine deaminase (AID), a potential RNA editing enzyme. *Cell.* 102:553–563. http://dx.doi.org/10.1016/S0092-8674(00)00078-7

Muto, A., K. Ochiai, Y. Kimura, A. Itoh-Nakadai, K.L. Calame, D. Ikebe, S. Tashiro, and K. Igarashi. 2010. Bach2 represses plasma cell gene regulatory network in B cells to promote antibody class switch. *EMBO J.* 29:4048–4061. http://dx.doi.org/10.1038/emboj.2010.257

Nelson, J.D., O. Denisenko, and K. Bomsztyk. 2006. Protocol for the fast chromatin immunoprecipitation (ChIP) method. *Nat. Protoc.* 1:179–185. http://dx.doi.org/10.1038/nprot.2006.27

Nguyen, H.V., E. Mouly, K. Chemin, R. Luinaud, R. Despres, J.P. Fermand, B. Arnulf, and J.C. Bories. 2012. The Ets-1 transcription factor is required for Stat1-mediated T-bet expression and IgG2a class switching in mouse B cells. *Blood.* 119:4174–4181. http://dx.doi.org/10.1182/blood-2011-09-378182

Oganesyan, G., S.K. Saha, E.M. Pietras, B. Guo, A.K. Miyahira, B. Zarnegar, and G. Cheng. 2008. IRF3-dependent type I interferon response in B cells regulates CpG-mediated antibody production. *J. Biol. Chem.* 283:802–808. http://dx.doi.org/10.1074/jbc.M704755200

Oliver, A.M., F. Martin, and J.F. Kearney. 1999. IgMhighCD21high lymphocytes enriched in the splenic marginal zone generate effector cells more rapidly than the bulk of follicular B cells. *J. Immunol.* 162:7198–7207.

Pasare, C., and R. Medzhitov. 2005. Control of B-cell responses by Toll-like receptors. *Nature.* 438:364–368. http://dx.doi.org/10.1038/nature04267

Peng, S.L., S.J. Szabo, and L.H. Glimcher. 2002. T-bet regulates IgG class switching and pathogenic autoantibody production. *Proc. Natl. Acad. Sci. USA.* 99:5545–5550. http://dx.doi.org/10.1073/pnas.082114899

Phan, T.G., S. Gardam, A. Basten, and R. Brink. 2005. Altered migration, recruitment, and somatic hypermutation in the early response of marginal zone B cells to T cell-dependent antigen. *J. Immunol.* 174:4567–4578. http://dx.doi.org/10.4049/jimmunol.174.8.4567

Pillai, S., A. Cariappa, and S.T. Moran. 2005. Marginal zone B cells. *Annu. Rev. Immunol.* 23:161–196. http://dx.doi.org/10.1146/annurev.immunol.23.021704.115728

Pilz, A., W. Kratky, S. Stockinger, O. Simma, U. Kalinke, K. Lingnau, A. von Gabain, D. Stoiber, V. Sexl, T. Kolbe, et al. 2009. Dendritic cells require STAT-1 phosphorylated at its transactivating domain for the induction of peptide-specific CTL. *J. Immunol.* 183:2286–2293. http://dx.doi.org/10.4049/jimmunol.0901383

Putz, E.M., D. Gotthardt, G. Hoermann, A. Csiszar, S. Wirth, A. Berger, E. Straka, D. Rigler, B. Wallner, A.M. Jamieson, et al. 2013. CDK8-mediated STAT1-S727 phosphorylation restrains NK cell cytotoxicity and tumor surveillance. *Cell Reports.* 4:437–444. http://dx.doi.org/10.1016/j.celrep.2013.07.012

Robertson, G., M. Hirst, M. Bainbridge, M. Bilenky, Y. Zhao, T. Zeng, G. Euskirchen, B. Bernier, R. Varhol, A. Delaney, et al. 2007. Genome-wide profiles of STAT1 DNA association using chromatin immunoprecipitation and massively parallel sequencing. *Nat. Methods.* 4:651–657. http://dx.doi.org/10.1038/nmeth1068

Saito, M., J. Gao, K. Basso, Y. Kitagawa, P.M. Smith, G. Bhagat, A. Pernis, L. Pasqualucci, and R. Dalla-Favera. 2007. A signaling pathway mediating downregulation of BCL6 in germinal center B cells is blocked by BCL6 gene alterations in B cell lymphoma. *Cancer Cell*. 12:280–292. http://dx.doi.org/10.1016/j.ccr.2007.08.011

Sciammas, R., A.L. Shaffer, J.H. Schatz, H. Zhao, L.M. Staudt, and H. Singh. 2006. Graded expression of interferon regulatory factor-4 coordinates isotype switching with plasma cell differentiation. *Immunity.* 25:225–236. http://dx.doi.org/10.1016/j.immuni.2006.07.009

Shaffer, A.L., X. Yu, Y. He, J. Boldrick, E.P. Chan, and L.M. Staudt. 2000. BCL-6 represses genes that function in lymphocyte differentiation, inflammation, and cell cycle control. *Immunity.* 13:199–212. http://dx.doi.org/10.1016/S1074-7613(00)00020-0

Shaffer, A.L., K.I. Lin, T.C. Kuo, X. Yu, E.M. Hurt, A. Rosenwald, J.M. Giltnane, L. Yang, H. Zhao, K. Calame, and L.M. Staudt. 2002. Blimp-1 orchestrates plasma cell differentiation by extinguishing the mature B cell gene expression program. *Immunity.* 17:51–62. http://dx.doi.org/10.1016/S1074-7613(02)00335-7

Shapiro-Shelef, M., and K. Calame. 2005. Regulation of plasma-cell development. *Nat. Rev. Immunol.* 5:230–242. http://dx.doi.org/10.1038/nri1572

Sharfe, N., A. Nahum, A. Newell, H. Dadi, B. Ngan, S.L. Pereira, J.A. Herbrick, and C.M. Roifman. 2014. Fatal combined immunodeficiency associated with heterozygous mutation in STAT1. *J. Allergy Clin. Immunol.* 133:807–817. http://dx.doi.org/10.1016/j.jaci.2013.09.032

Song, H., and J. Cerny. 2003. Functional heterogeneity of marginal zone B cells revealed by their ability to generate both early antibody-forming cells and germinal centers with hypermutation and memory in response to a T-dependent antigen. *J. Exp. Med.* 198:1923–1935. http://dx.doi.org/10.1084/jem.20031498

Staab, J., C. Herrmann-Lingen, and T. Meyer. 2013. CDK8 as the STAT1 serine 727 kinase? *JAK-STAT.* 2:e24275. http://dx.doi.org/10.4161/jkst.24275

Swanson, C.L., T.J. Wilson, P. Strauch, M. Colonna, R. Pelanda, and R.M. Torres. 2010. Type I IFN enhances follicular B cell contribution to the T cell-independent antibody response. *J. Exp. Med.* 207:1485–1500. http://dx.doi.org/10.1084/jem.20092695

Tanigaki, K., H. Han, N. Yamamoto, K. Tashiro, M. Ikegawa, K. Kuroda, A. Suzuki, T. Nakano, and T. Honjo. 2002. Notch-RBP-J signaling is involved in cell fate determination of marginal zone B cells. *Nat. Immunol.* 3:443–450. http://dx.doi.org/10.1038/ni793

Thibault, D.L., A.D. Chu, K.L. Graham, I. Balboni, L.Y. Lee, C. Kohlmoos, A. Landrigan, J.P. Higgins, R. Tibshirani, and P.J. Utz. 2008. IRF9 and STAT1 are required for IgG autoantibody production and B cell expression of TLR7 in mice. *J. Clin. Invest.* 118:1417–1426. http://dx.doi.org/10.1172/JCI30065

Thibault, D.L., K.L. Graham, L.Y. Lee, I. Balboni, P.J. Hertzog, and P.J. Utz. 2009. Type I interferon receptor controls B-cell expression of nucleic acid-sensing Toll-like receptors and autoantibody production in a murine model of lupus. *Arthritis Res. Ther.* 11:R112. http://dx.doi.org/10.1186/ar2771

Tunyaplin, C., M.A. Shapiro, and K.L. Calame. 2000. Characterization of the B lymphocyte-induced maturation protein-1 (Blimp-1) gene, mRNA isoforms and basal promoter. *Nucleic Acids Res.* 28:4846–4855. http://dx.doi.org/10.1093/nar/28.24.4846

Tunyaplin, C., A.L. Shaffer, C.D. Angelin-Duclos, X. Yu, L.M. Staudt, and K.L. Calame. 2004. Direct repression of prdm1 by Bcl-6 inhibits plasmacytic differentiation. *J. Immunol.* 173:1158–1165. http://dx.doi.org/10.4049/jimmunol.173.2.1158

Varinou, L., K. Ramsauer, M. Karaghiosoff, T. Kolbe, K. Pfeffer, M. Müller, and T. Decker. 2003. Phosphorylation of the Stat1 transactivation domain is required for full-fledged IFN-gamma-dependent innate immunity. *Immunity.* 19:793–802. http://dx.doi.org/10.1016/S1074-7613(03)00322-4

Vasanwala, F.H., S. Kusam, L.M. Toney, and A.L. Dent. 2002. Repression of AP-1 function: a mechanism for the regulation of Blimp-1 expression and B lymphocyte differentiation by the B cell lymphoma-6 protooncogene. *J. Immunol.* 169:1922–1929. http://dx.doi.org/10.4049/jimmunol.169.4.1922

Wallick, S., J.L. Claflin, and D.E. Briles. 1983. Resistance to Streptococcus pneumoniae is induced by a phosphocholine-protein conjugate. *J. Immunol.* 130:2871–2875.

Wang, W.B., D.E. Levy, and C.K. Lee. 2011. STAT3 negatively regulates type I IFN-mediated antiviral response. *J. Immunol.* 187:2578–2585. http://dx.doi.org/10.4049/jimmunol.1004128

Whitlock, C.A., and J.D. Watson. 1979. B-cell differentiation in the CBA/N mouse. I. Slower maturation of mitogen and antigen-responsive B cells in mice expressing an X-linked defect. *J. Exp. Med.* 150:1483–1497. http://dx.doi.org/10.1084/jem.150.6.1483

Xu, W., and J.J. Zhang. 2005. Stat1-dependent synergistic activation of T-bet for IgG2a production during early stage of B cell activation. *J. Immunol.* 175:7419–7424. http://dx.doi.org/10.4049/jimmunol.175.11.7419